Conductive Path Formation in the Ta_2O_5 Atomic Switch: First-Principles Analyses

Tingkun Gu,* Tomofumi Tada, and Satoshi Watanabe

Department of Materials Engineering, The University of Tokyo, Tokyo 113-8656, Japan

ARTICLE

ABSTRACT The conductive path formed by the interstitial Cu or oxygen vacancies in the Ta_2O_5 atomic switch were investigated in detail by first-principles methods. The calculated results indicated that the defect state induced by the interstitial Cu is located just at the Fermi level of the Cu and Pt electrodes in the Cu/Ta_2O_5/Pt heterostructure and that a conduction channel is formed in the Ta_2O_5 film *via* the interstitial Cu. On the other hand, oxygen vacancies in Ta_2O_5 do not form such a conduction channel because of the lower energy positions of their defect states. The above results suggest that the conductive path could be formed by interstitial Cu in the Ta_2O_5 atomic switch, whereas the oxygen vacancies do not contribute to the formation of the conductive path.

KEYWORDS: atomic switch · tantalum pentoxide · first-principles simulation · transport properties · conductive path · schottky barrier

The nanoscale resistive switch is a promising key element in both logic and memory circuits and gained considerable attention recently. By controlling individual atoms in a quantum point contact or metallic filament in solid electrolyte, several types of atomic switches have been fabricated in recent years.[1−4] Among these, atomic switches based on metal−insulator−metal (MIM) systems have attracted considerable attention due to their high scalability and the prospect of low power consumption in device applications, such as nonvolatile memory. These switches can be divided into two groups, namely, unipolar switches, in which both writing and erasing occur with the same voltage polarity, and bipolar switches, in which the set and reset operations require the polarities of the applied voltage to be opposite one another.[5] Bipolar switches are usually designed with an asymmetric structure, in which the insulator is sandwiched between an oxidizable electrode, such as Ag or Cu, and an inert electrode, such as Pt or Au. Intermediate insulators used in previously reported experiments include chalcogenides, such as Ge_xSe_{1-x},[6,7] Cu_2S,[8] and Ag_2S,[4] as well as oxides, such as WO_3,[9] SiO_2,[10] and Ta_2O_5.[11]

In the present study, we focus on a bipolar switch with Ta_2O_5, which is particularly promising as a practical device because of its compatibility with semiconductor fabrication processes. The mechanism of the bipolar switches appears to be understood primarily on the basis of the electrochemical redox reaction: the applied bias voltage causes the migration of metal ions in the insulating solid-electrolyte layer between metal electrodes and induces metal precipitation, which serves as a conduction channel in the high-conductance (low-resistance) state of the switches. The atomistic details of the mechanism of the atomic switches, however, are not understood sufficiently, and so we have been examining these using first-principles methods. Thus far, we have studied MIM systems with insulator layers of Ag_2S,[12,13] assuming that excess Ag precipitated into Ag_2S following the experimental observation.[14] In the case of the Ta_2O_5 atomic switch, composition analyses of Ta_2O_5 film before and after applying a voltage showed that the Cu ions migrated from the Cu electrode into the Ta_2O_5 film, supporting the assumption of a conducting Cu filament in Ta_2O_5.[11] However, detailed information on the microstructure of this Cu filament, in particular its thinnest part, which would be crucial in the transition between high- and low-conductance states, is still lacking.

In the present study, we examine the atomic and electronic structures of Ta_2O_5 with interstitial Cu and its effects on the transport properties of heterostructure Cu/Ta_2O_5/Pt by first-principles methods in an attempt to understand the mechanism of the atomic switch. In addition, we also examine oxygen vacancies in Ta_2O_5, because

*Address correspondence to gutk@sdu.edu.cn.

Received for review June 22, 2010 and accepted October 04, 2010.

Published online October 8, 2010.
10.1021/nn101410s

© 2010 American Chemical Society

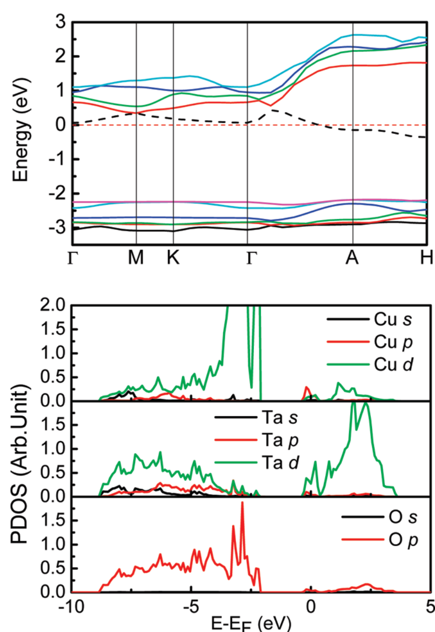

Figure 1. Energy band structure (top) and projected density of states (bottom) of Ta_2O_5 with an interstitial Cu. The dashed line in the top panel denotes the defect state induced by the interstitial Cu.

oxygen vacancies are often considered to play an important role in resistive switches. We will demonstrate that in the Ta_2O_5 atomic switch, the interstitial Cu forms a conduction path, whereas oxygen vacancies do not.

RESULTS AND DISCUSSION

Bulk Ta_2O_5 with Cu Interstitials or Oxygen Vacancies. In examining the interstitial Cu, we assume δ-Ta_2O_5 phase for the bulk Ta_2O_5, which is energetically the most stable.[15] Careful analysis of the crystal structure of δ-Ta_2O_5 reveals that there is one interstitial position in the Ta−O plane (2*c* site) and three interstitial positions in the O plane (2*d*, 6*m*, and 6*k*). The formation energies of the interstitial Cu inserted in these four types of positions were calculated using a unit cell consisting of 10 O atoms, 4 Ta atoms, and 1 Cu atom while relaxing the unit cell volume and atomic position. The calculated formation energies were −1.06, −0.63, −0.62, and 3.63 eV for 6*k*, 6*m*, 2*d*, and 2*c*, respectively. Thus, the most stable structure for one unit cell of Ta_2O_5 with one interstitial Cu is found to be Cu at the 6*k* site.

Figure 1 shows the projected density of states (PDOS) and energy band structure of the Ta_2O_5 with an interstitial Cu at 6*k*. The Cu atom inserted at 6*k* induces an energy band across the Fermi level, which is located just below the conduction band of the pure δ-Ta_2O_5. The PDOS reveals that this defect state consists of Ta (*d*) and Cu (*p*, *d*) components. The Ta (*d*) component in this state is much larger than that of Cu (*p*, *d*), which is partly because a part of this state (*e.g.*, the region along the *M*-*K*-Γ line) is actually the conduction band of Ta_2O_5. Note also that most of the Cu (*p*, *d*) component is in resonance near the top of the valence band. Figure 2 shows the isosurface of partial charge density for the defect state near the Fermi level, which is the charge density of the energy band indicated by the dashed line in Figure 1. Interestingly, a connective path is formed between two adjacent Ta−O planes *via* the interstitial Cu. Here, we would like to emphasize that the density of the interstitial Cu in this calculation is rather high, that is, one Cu per unit cell of δ-Ta_2O_5. When the Cu density is lower, there are several possible alignments of the interstitial Cu atoms in Ta_2O_5. We examined this point using a supercell consisting of five unit cells of δ-Ta_2O_5 stacked along the [001] direction. The following four models were examined. In model A, a supercell contains only one interstitial Cu. In model B (hereinafter referred to as the direct path), the alignment of the interstitial Cu atoms is the same as that in the case of one Cu per unit cell. In model C (hereinafter referred to as the defective path), one Cu atom is removed from the direct path. In model D (hereinafter referred to as the deformed path), one interstitial Cu in the direct path moves to the adjacent 6*k* site in the same O plane. The isosurfaces of partial charge corresponding to the defect states for these four models are shown in Figure 3 and are calculated in the same manner as in Figure 2. Although the connection of two adjacent Ta−O planes *via* the interstitial Cu is observed in all four models, a perfect connective path from one side of the supercell to the other is formed only in the case of the direct path. Therefore, we speculate that only the direct path contributes to the electronic transport of Ta_2O_5 film in the heterojunction of Cu/Ta_2O_5/Pt.

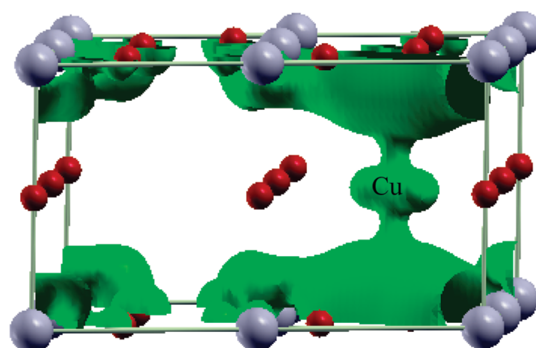

Figure 2. Isosurface plot of the partial charge density corresponding to the defect state induced by the interstitial Cu (see Figure 1) in Ta_2O_5 at 0.04 e/Å^3. Smaller and larger balls denote O and Ta atoms, respectively.

There are three oxygen vacancies in δ-Ta_2O_5, located at 6*l*, 3*g*, and 1*b* sites.[15] The calculated formation energies for these three oxygen vacancies are 2.88, 5.01, and 6.77 eV for 6*l*, 3*g*, and 1*b*, respectively. The positive values of formation energy indicate that none of the oxygen vacancies are stable in Ta_2O_5. Although this suggests the possibility, albeit slight, of conduction paths formed by oxygen vacancy in Ta_2O_5, it would be worthwhile to compare states induced by oxygen vacancy with those induced by interstitial Cu. Therefore, we examine the energy band structure and projected

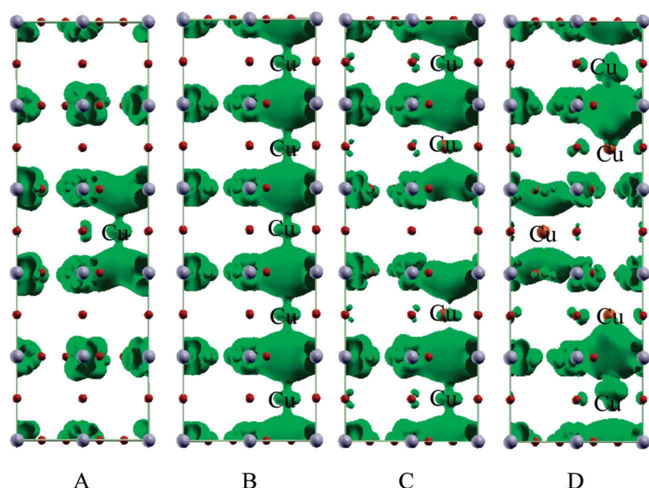

Figure 3. Isosurface plot of the partial charge density corresponding to the defect states for Ta_2O_5 with a single interstitial Cu (A), direct path Cu (B), defective path Cu (C), and deformed path Cu (D) at 0.04 e/Å^3. Smaller and larger balls correspond to O and Ta, respectively.

high-conductance states in the heterostructure as well as the formation of the conduction channel in the Ta_2O_5. For this purpose, a heterostructure Cu/Ta_2O_5/Pt model was adopted. The details of the model and method are the same as those adopted in our previous study on the Cu/pure-Ta_2O_5/Pt,[15] and the barrier heights were evaluated using the bulk-plus-lineup method.[16−18] Figure 6 shows the electrostatic potential averaged on the $x-y$ plane, that is, planar average potential, and the macroscopic average potential obtained by averaging the planar average potential over the periodicity lengths along the z-direction for Cu (or Pt) and Ta_2O_5. Here, the z-direction is the direction perpendicular to the interface. The evaluated Schottky barrier height (the minimum edge of the defect state with respect to the Fermi level) is in the range of -0.08 to $+0.28$ eV as the Cu path in Ta_2O_5 film, whereas for oxygen vacancies, this value (the maximum edge of the defect state with respect to the Fermi level) is in the range of -1.18 to -0.40 eV (see Figure 6). Here, the range of evaluated values is based on the fact that the average of the effective potential in the plane parallel to the interface varies considerably with the position in the Ta_2O_5 layer. The evaluated Schottky barrier height also suggests that the paths formed by interstitial Cu atoms may be highly conductive.

density of states for the most stable oxygen vacancy, that is, that at 6*l*, as shown in Figure 4. One energy band appears in the band gap of δ-Ta_2O_5, and its energy position is much lower than that of the band induced by the interstitial Cu. Further analyses reveal that the partial charge density corresponding to the vacancy-induced states is localized around the vacancy site (see Figure 5), in contrast to the case of the Cu-interstitial-induced states. Again, this feature of the oxygen-vacancy-induced states suggests the slight possibility of conduction paths being formed by oxygen vacancy in Ta_2O_5.

Schottky Barrier in the Heterostructure of Cu/Ta_2O_5/Pt. Next, we examined the effects of interstitial Cu on Schottky barrier in the heterostructure of Cu/Ta_2O_5/Pt, because a low Schottky barrier is a necessary conduction for the

Transport Properties of Heterostructure Cu/Ta_2O_5/Pt. All of the models in this calculation contain four O planes and three Ta−O planes of Ta_2O_5 arranged alternatively. Semi-infinite Cu and Pt electrodes are considered: three Cu layers and three Pt layers are taken into account explicitly, while other layers are considered in the form of self-energies. First, we examine two models, Cu/Ta_2O_5/Pt with interstitial Cu atoms in the direct path arrangement and Cu/Ta_2O_5/Pt with oxygen vacancies in the direct path arrangement. The calculated transmission spectra for these models are shown in the bottom panel of Figure 7. As reported in our previous paper,[15]

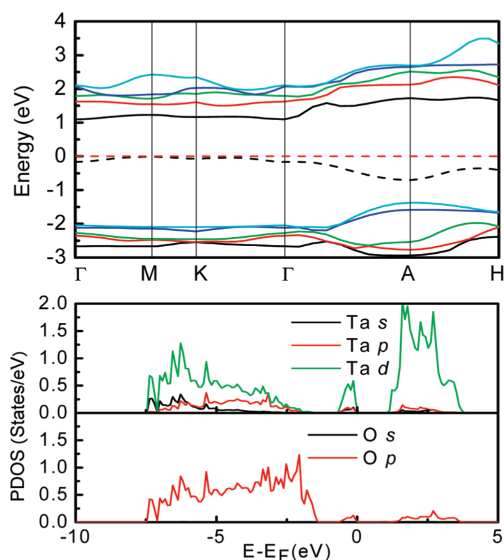

Figure 4. Energy band structure (top) and projected density of states (bottom) of Ta_2O_5 with an oxygen vacancy. The dashed line in the top panel denotes the defect state induced by the oxygen vacancy.

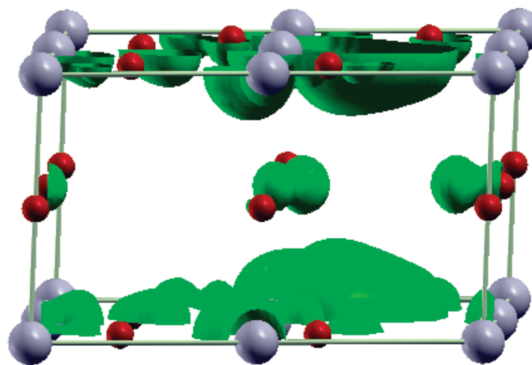

Figure 5. Isosurface plot of the partial charge density corresponding to the defect state induced by the oxygen vacancy (see Figure 4) in Ta_2O_5 at 0.04 e/Å^3. The smaller and larger balls denote O and Ta atoms, respectively.

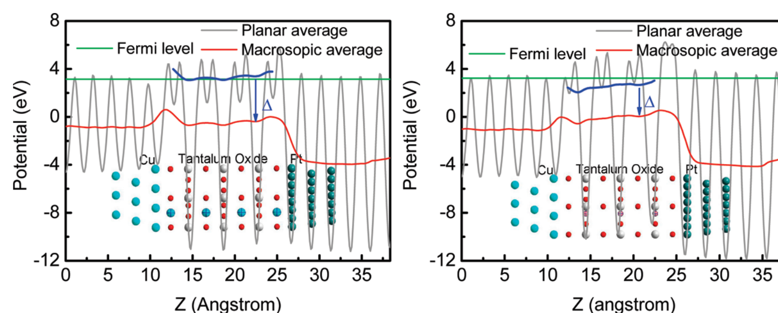

Figure 6. Planar and macroscopic average of the electrostatic potential calculated from the relaxed Cu/Ta_2O_5/Pt heterostructure. (Left) Ta_2O_5 with interstitial Cu. (Right) Ta_2O_5 with oxygen vacancies. Turquoise balls, Cu; red balls, O; gray balls, Ta; light blue balls, Pt. The symbol Δ indicates the lowest energy level of the defect state for the interstitial Cu and the largest energy level of the defect state for the oxygen vacancy relative to the reference potential.

the transmission spectrum of Cu/Ta_2O_5/Pt without defects has a wide zero-transmission basin in the energy range from −0.8 to 0.5 eV, which indicates that the Fermi level of metal electrodes is just pinned in the band gap of Ta_2O_5 and that no conduction channels for current flow are formed in Ta_2O_5 film. The transmission spectrum of the heterostructure with the direct path of oxygen vacancies also has a wide zero-transmission basin, but has a small peak at −0.4 eV, which corresponds to the midgap states induced by oxygen vacancies, as mentioned previously. Because of this peak, a slightly larger electronic conduction is expected in the heterostructure with the direct path of oxygen vacancies, as compared to the heterostructure without vacancies. As for the heterostructure with the direct path of interstitial Cu atoms, a notable peak appears around the Fermi level, which suggests much larger conduction in this system, as compared to the other two systems. The calculated current−voltage curves confirm the above features of conduction suggested by the transmission spectra. For example, at a bias voltage of 0.6 V, a much larger current (7.65 μA) flows in the heterostructure with the direct path of interstitial Cu atoms, as compared to the other two cases (0.28 μA in the direct path of oxygen vacancies and 0.12 μA in the pure Ta_2O_5).

Next, we examined the electronic conduction in the heterostructures with the deformed and defective paths of interstitial Cu atoms. The calculated transmission spectra for these two cases are also shown in Figure 7. In both cases, a wide zero-transmission basin appears around the Fermi level in the transmission curve. Correspondingly, the local density of states at the Fermi level, which are shown in Figure 8 for the defective path case, lack a high-density bridge connecting the two electrodes, which is in contrast to the case of the direct path (also shown in Figure 8). Based on these results, the transport properties of Cu/δ-Ta_2O_5/Pt heterostructures with interstitial Cu atoms in the Ta_2O_5 layer are quite sensitive to the arrangement of the interstitial atoms.

DISCUSSION

Finally, we would like to discuss the mechanism of the Ta_2O_5 atomic switch based on the calculated results mentioned above. According to the experimental results, Cu atoms migrate from the Cu electrode into the Ta_2O_5 film when a positive voltage is applied to the

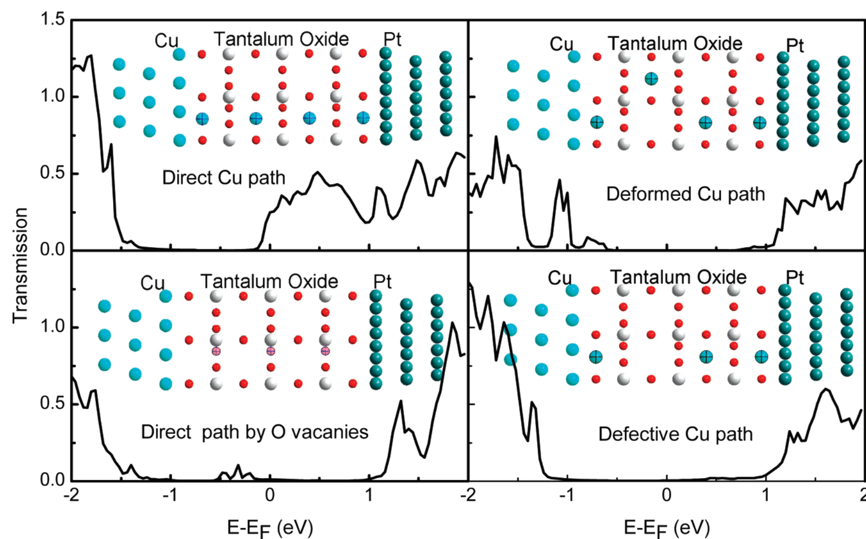

Figure 7. Transmission spectra of heterostructure Cu/Ta_2O_5/Pt for different models. In the Ta_2O_5 slab, the interstitial Cu and O vacancy atoms are denoted by balls with crosses, and O and Ta atoms are denoted by smaller and larger balls, respectively.

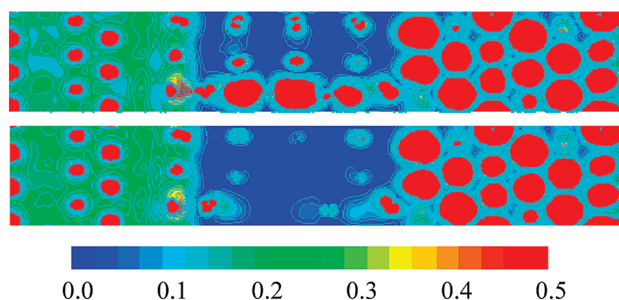

Figure 8. Contour plot of spatially resolved density of states (units: $1/\mathrm{Bohr}^{3/2}$) projected onto the *x-y* plane along the transport direction in $Cu/Ta_2O_5/Pt$ heterostructures with the direct Cu path (top) and the defective Cu path (bottom).

Cu electrode. For the case in which considerable numbers of Cu atoms precipitate into the Ta_2O_5, the precipitation region would exhibit properties similar to those of bulk Cu. In this case, such a region serves as a conduction channel. However, even in such a case, the properties and the atomic structure of this small region, which is crucial in the switching between high- and low-conductance states, may be different from those of bulk Cu. Our study would give us hints for the small region. The calculated results reveal that high-conductance paths can be formed by interstitial (but not precipitated) Cu atoms in Ta_2O_5, such as the direct path of interstitial Cu atoms. Note that, in the above models, the calculated formation energies of the direct and deformed paths of Cu interstitials are -1.06 and -0.87 eV per Cu atom, respectively. Thus, from the viewpoint of energetic stability, the more conductive direct path of Cu is more stable than the less conductive deformed path. On the other hand, there is a high possibility that even in the extremely small Ta_2O_5 atomic switch, switching between high- and low-conductance states requires at least several atoms, as shown for the case of the Ag_2S atomic switch.[13] Note also that the results of the present study preclude the possibility of conduction path formation by oxygen vacancy. This is in sharp contrast with other resistive switching systems, such as TiO_2 switching systems.[19,20]

CONCLUSION

We have examined the effects of interstitial Cu and oxygen vacancies on the electronic structure of δ-Ta_2O_5 and the transport properties of $Cu/Ta_2O_5/Pt$ heterostructure. We found that two adjacent Ta−O planes are connected *via* the Cu interstitial in the partial charge density of the defect state in the unit cell of δ-Ta_2O_5. Furthermore, the energy position of the defect states is nearly the same as the Fermi levels of the Cu and Pt electrodes in the $Cu/Ta_2O_5/Pt$ heterostructure, and a row of interstitial Cu atoms in the direction normal to the Ta−O planes forms a conducting channel in the Ta_2O_5 layer. Electronic conduction through the interstitial Cu atoms is sensitive to the arrangement of the interstitials. On the other hand, oxygen vacancies in Ta_2O_5 do not contribute to the formation of conducting channels.

METHODS

All of the calculations for the electronic structures of bulk Ta_2O_5 with interstitial Cu or oxygen vacancies were performed using the Vienna *ab initio* simulation package (VASP).[21,22] A plane wave basis set with a cutoff energy of 400.0 eV was used. The projector augmented-wave (PAW)[23] method and the generalized gradient approximation (PW91)[24] were used to describe the electron-ion and electron−electron interactions, respectively. The computational conditions were the same as those adopted in our previous study on the atomic and electronic structure of bulk Ta_2O_5.[15]

Next, the following equation was used to obtain the macroscopic average potential, $f_M(z)$, shown in Figure 6:

$$f_M(z) = \int dz' \int dz'' \, \omega_{l1}(z - z') \, \omega_{l2}(z' - z'') \, f_P(z'')$$

where

$$\omega_l(z) = \frac{1}{l}\Theta\left(\frac{l}{2} - |z|\right)$$

is the filtering function, Θ is the one-dimensional step function, and $f_P(z)$ is the potential averaged in the directions parallel to the interface (planar average potential on the *x-y* plane). The characteristic lengths $l1$ and $l2$ are half the lattice constant of metallic Cu and half the lattice constant of Ta_2O_5, respectively. Note that we also used these parameters for the Pt electrodes. We confirmed that the results change only slightly if the Pt lattice constant is adopted instead of the Cu lattice constant, because the difference between the two lattice constants is small.

Finally, the electronic transport properties of heterostructures $Cu/Ta_2O_5/Pt$ in which the Ta_2O_5 slab contained interstitial Cu or oxygen vacancies were examined using the Atomistix Toolkit (ATK) program based on the density functional theory and nonequilibrium Green's function method. The computational conditions were the same as those adopted in our previous study.[15]

Acknowledgement The present study was supported in part by a Grant-in-Aid for Scientific Research on Priority Area, "Nanoionics (439)", a Grant-in-Aid for Key-Technology, "Atomic Switch Programmed Device", and by the Global COE Program "Global Center of Excellence for Mechanical Systems Innovation" through the Ministry of Education, Culture, Sports, Science and Technology of Japan. S. Watanabe would like to thank S. Yamaguchi, T. Sakamoto, and N. Banno for stimulating discussions.

REFERENCES AND NOTES

1. Xie, F. Q.; Maul., R.; Augenstein, A.; Obermair, Ch.; Starikov, E. B.; Schön, G.; Schimmel, Th.; Wenzel, W. Independently Switchable Atomic Quantum Transistors by Reversible Contact Reconstruction. *Nano Lett.* **2008**, *8*, 4493–4497.
2. Xie, F. Q.; Maul, R.; Obermair, Ch.; Schön, G.; Schimmel, Th.; Wenzel, W. Multilevel Atomic-Scale Transistors Based on Metallic Quantum Point Contacts. *Adv. Mater.* **2010**, *22*, 2033–2036.
3. Martin, C. A.; Smit, R. H. M.; van der Zant, H. S. J.; van Ruitenbeek, J. M. A Nanoelectromechanical Single-Atom Switch. *Nano Lett.* **2009**, *9*, 2940–2945.

4. Terabe, K.; Hasegawa, T.; Nakayama, T.; Aono, M. Quantized Conductance Atomic Switch. *Nature* **2005**, *433*, 47–50.
5. Waser, R.; Aono, M. Nanoionics-Based Resistive Switching Memories. *Nat. Mater.* **2007**, *6*, 833–840.
6. Kozicki, M. N.; Park, M.; Mitkova, M. Nanoscale Memory Elements Based on Solid-State Electrolytes. *IEEE Trans. Nanotechnol.* **2005**, 331–338.
7. Mitkova, M.; Kozicki, M. N. Silver Incorporation in Ge−Se Glasses Used in Programmable Metallization Cell Devices. *J. Non-Cryst. Solids.* **2002**, *299*−*302*, 1023–1027.
8. Sakamoto, T.; Sunamura, H.; kawaura, H.; Hasegawa, T.; Nakayama, T.; Aono, M. Nanometer-Scale Switches Using Copper Sulfide. *Appl. Phys. Lett.* **2003**, *82*, 3032–3034.
9. Kozicki, M. N.; Gopalan, C.; Balakrishnan, M.; Mitkova, M. A Low-Power Nonvolatile Switching Element Based on Copper-Tungsten Oxide Solid Electrolyte. *IEEE Trans. Nanotechnol.* **2006**, *5*, 535–544.
10. Schindler, C.; Thermadam, S. C. P.; Waser, R.; Kozicki, M. N. Bipolar and Unipolar Resistive Switching in Cu-Doped SiO_2. *IEEE Trans. Electron Devices* **2007**, *54*, 2762–2768.
11. Sakamoto, T.; Lister, K.; Banno, N.; Hasegawa, T.; Terabe, K.; Aono, M. Electronic Transport in Ta_2O_5 Resistive Switch. *Appl. Phys. Lett.* **2007**, *91*, 092110.
12. Wang, Z. C.; Kadohira, T.; Tada, T.; Watanabe, S. Nonequilibrium Quantum Transport Properties of a Silver Atomic Switch. *Nano Lett.* **2007**, *7*, 2688–2692.
13. Wang, Z. C.; Gu, T. K.; Tada, T.; Watanabe, S. Excess-Silver-Induced Bridge Formation in a Silver Sulfide Atomic Switch. *Appl. Phys. Lett.* **2008**, *93*, 152106.
14. Kundu, M.; Terabe, K.; Hasegawa, T.; Aono, M. Effect of Sulfurization Conditions and Post-Deposition Annealing Treatment on Structural and Electrical Properties of Silver Sulfide Films. *J. Appl. Phys.* **2006**, *99*, 103501.
15. Gu, T. K.; Wang, Z. C.; Tada, T.; Watanabe, S. First-Principles Simulations on Bulk Ta_2O_5 and $Cu/Ta_2O_5/Pt$ Heterojunction: Electronic Structures and Transport Properties. *J. Appl. Phys.* **2009**, *106*, 103713.
16. Van de Walle, C. G.; Martin, R. M. Theoretical Calculations of Heterojunction Discontinuities in the Si/Ge System. *Phys. Rev. B* **1986**, *34*, 5621–5634.
17. Peressi, M.; Binggeli, N.; Baldereschi, A. Band Engineering at Interfaces: Theory and Numerical Experiments. *J. Phys. D* **1998**, *31*, 1273–1299.
18. Wei, S. H.; Zunger, A. Role of d Orbitals in Valence-Band Offsets of Common-Anion Semiconductors. *Phys. Rev. Lett.* **1987**, *59*, 144.
19. Yang, J. J.; Pickett, M. D.; Stewart, D. R.; Li, X.; Ohlberg, A. A. D.; Stewart, D. R. Memristive Switching Mechanism for Metal/Oxide/Metal Nanodevices. *Nat. Nanotechnol.* **2008**, *3*, 429–433.
20. Jeong, H. Y.; Lee, J. Y.; Choi, S.-Y.; Kim, J. W. Microscopic Origin of Bipolar Switching of Nanoscale Titanium Oxide Thin Films. *Appl. Phys. Lett.* **2009**, *95*, 162108.
21. Kresse, G.; Furthmüller, J. Efficiency of *ab-Initio* Total Energy Calculations for Metals and Semiconductors Using a Plane-Wave Basis Set. *Comput. Mater. Sci.* **1996**, *6*, 15–50.
22. Kresse, G.; Furthmüller, J. Efficient Iterative Schemes for *ab Initio* Total-Energy Calculations Using a Plane-Wave Basis Set. *Phys. Rev. B* **1996**, *54*, 11169–11186.
23. Kresse, G.; Joubert, J. From Ultrasoft Pseudopotentials to the Projector Augmented-Wave Method. *Phys. Rev. B* **1999**, *59*, 1758–1775.
24. Wang, Y.; Perdew, J. P. Correlation Hole of the Spin-Polarized Electron Gas, with Exact Small-Wave-Vector and High-Density Scaling. *Phys. Rev. B* **1991**, *44*, 13298–13307.